

## Microbial Manganese and Sulfate Reduction in Black Sea Shelf Sediments

BO THAMDRUP,<sup>1,2\*</sup> RAMÓN ROSSELLÓ-MORA,<sup>1†</sup> AND RUDOLF AMANN<sup>1</sup>

Max Planck Institute for Marine Microbiology, Bremen, Germany,<sup>1</sup> and Danish Center for Earth System Science, Institute of Biology, SDU—Odense University, Odense, Denmark<sup>2</sup>

Received 29 February 2000/Accepted 5 May 2000

**The microbial ecology of anaerobic carbon oxidation processes was investigated in Black Sea shelf sediments from mid-shelf with well-oxygenated bottom water to the oxic-anoxic chemocline at the shelf-break. At all stations, organic carbon (C<sub>org</sub>) oxidation rates were rapidly attenuated with depth in anoxically incubated sediment. Dissimilatory Mn reduction was the most important terminal electron-accepting process in the active surface layer to a depth of ~1 cm, while SO<sub>4</sub><sup>2-</sup> reduction accounted for the entire C<sub>org</sub> oxidation below. Manganese reduction was supported by moderately high Mn oxide concentrations. A contribution from microbial Fe reduction could not be discerned, and the process was not stimulated by addition of ferrihydrite. Manganese reduction resulted in carbonate precipitation, which complicated the quantification of C<sub>org</sub> oxidation rates. The relative contribution of Mn reduction to C<sub>org</sub> oxidation in the anaerobic incubations was 25 to 73% at the stations with oxic bottom water. In situ, where Mn reduction must compete with oxygen respiration, the contribution of the process will vary in response to fluctuations in bottom water oxygen concentrations. Total bacterial numbers as well as the detection frequency of bacteria with fluorescent in situ hybridization scaled to the mineralization rates. Most-probable-number enumerations yielded up to 10<sup>5</sup> cells of acetate-oxidizing Mn-reducing bacteria (MnRB) cm<sup>-3</sup>, while counts of Fe reducers were <10<sup>2</sup> cm<sup>-3</sup>. At two stations, organisms affiliated with *Arcobacter* were the only types identified from 16S rRNA clone libraries from the highest positive MPN dilutions for MnRB. At the third station, a clone type affiliated with *Pelobacter* was also observed. Our results delineate a niche for dissimilatory Mn-reducing bacteria in sediments with Mn oxide concentrations greater than ~10 μmol cm<sup>-3</sup> and indicate that bacteria that are specialized in Mn reduction, rather than known Mn and Fe reducers, are important in this niche.**

The complete oxidation of organic compounds through the dissimilatory reduction of Mn or Fe oxide constitutes the most recently discovered and least explored of the major types of anaerobic respiration in nature (34). Over recent years, bacteria and archaea that carry out these types of metabolism have been found in many different environments, and a large phylogenetic and metabolic diversity is becoming evident (35, 70). Also, a basic understanding of the ecological niches of Mn- and Fe-reducing organisms has emerged. In natural environments, the occurrence of Mn and Fe reduction has been found to depend primarily on the presence of Mn oxide and poorly crystalline Fe oxide, respectively. Thus, when Mn oxide is abundant under anoxic conditions, microbial Mn reduction dominates carbon oxidation over Fe and sulfate reduction (10, 38, 47). When Mn oxides are absent and enough poorly crystalline Fe(III) is available, Fe reduction dominates over sulfate reduction (13, 39, 65). This sequence can be explained through differences between the metabolic types in their efficiency of competition for common substrates (36, 37).

The first determinations of the processes in natural environments have shown that dissimilatory Mn or Fe reduction may, under certain circumstances, dominate carbon oxidation in both marine and freshwater sediments (13, 54). Microbial Fe reduction is an important process in many aquatic sediments. In a recent compilation, Fe reduction contributed 22% on average to anaerobic carbon oxidation in 16 different conti-

mental margin sediments, with the rest being primarily coupled to sulfate reduction (65). In contrast, organotrophic microbial Mn reduction has only been identified in two offshore basins, the Panama Basin and the Norwegian Trough, characterized by extremely high Mn oxide contents, where Mn reduction was the most important carbon oxidation pathway (2, 10). In coastal sediments, microbial Mn reduction is generally concluded to be of little significance in carbon oxidation, due to a relatively low abundance and shallow vertical penetration of Mn oxides, although studies of microbial Mn reduction are often hampered by the spatial resolution of available techniques (65). Because the sedimentation of Mn and Fe oxides to most sediments is much smaller than the benthic carbon oxidation rate, an efficient recycling of reduced Mn and Fe must take place when levels of Mn and Fe reduction are significant in carbon oxidation (13). The reoxidation of reduced Mn and Fe is stimulated by bioturbation through particle mixing or pore-water irrigation, and this Mn and Fe cycling ultimately depends on the presence of oxygen in the bottom water (2, 13).

A detailed understanding of the regulation of Mn and Fe reduction in sediments includes knowledge of the quantitatively important Mn- and Fe-reducing bacteria. However, the size and composition of the Mn- and Fe-reducing microbial communities in marine sediments are virtually unknown. With few exceptions, reduction of Mn and Fe is catalyzed by the same cultivated organisms (35), but most of these were enriched on Fe oxide, and the existence of specialized Mn reducers has been poorly investigated. Some sulfate-reducing bacteria which also couple carbon oxidation to Fe oxide reduction could also contribute to benthic Fe reduction (17, 40), although dissimilatory Fe reduction was not observed after addition of poorly crystalline Fe oxide to a sulfate-reducing

\* Corresponding author. Mailing address: Institute of Biology, Odense University, Campusvej 55, DK-5230 Odense M, Denmark. Phone: 45 65502477. Fax: 45 65930457. E-mail: bot@biology.sdu.dk.

† Present address: Laboratori de Microbiologia, Facultat de Ciències, Universitat de les Illes Balears, Palma de Mallorca, Spain.

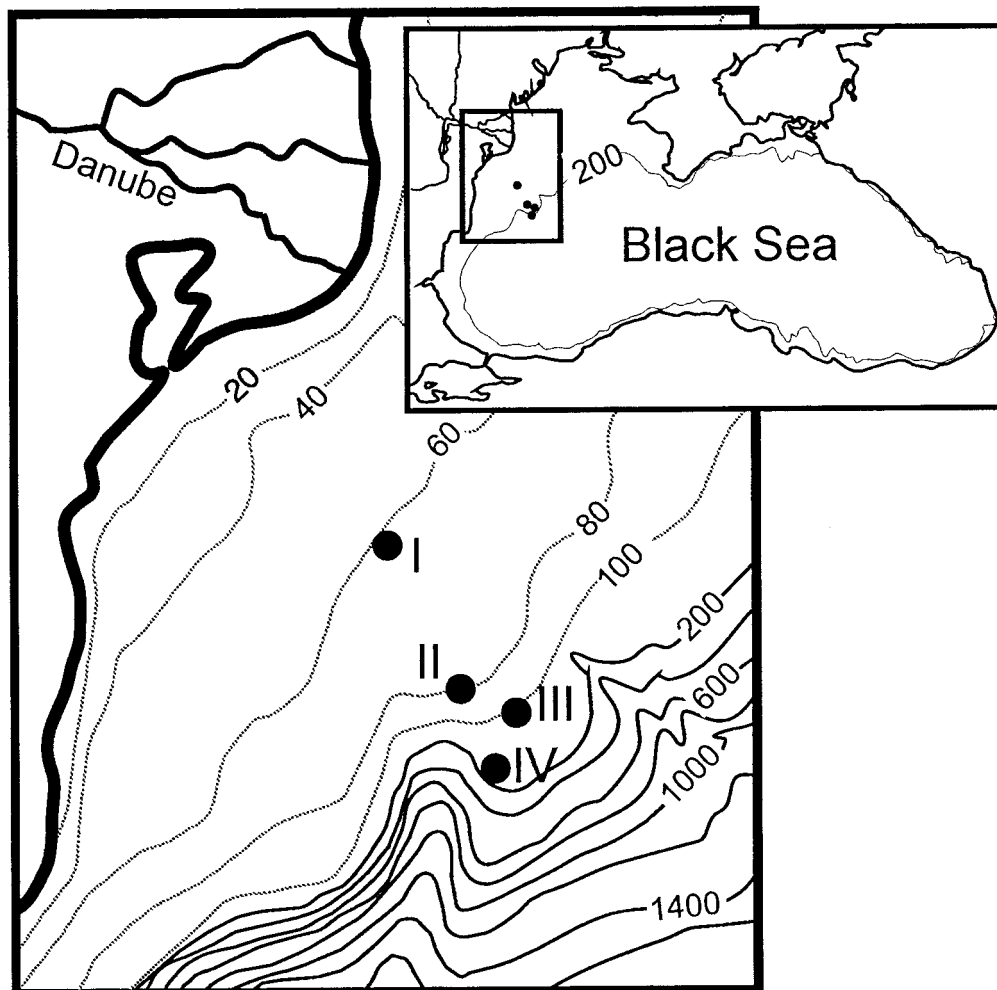


FIG. 1. Maps of the Black Sea and the study area on the Romanian shelf. The numbers indicate water depth (meters).

coastal sediment (15). In this sediment, most-probable-number (MPN) counts furthermore yielded 1,000-fold-fewer Fe-reducing than sulfate-reducing bacteria, and this relationship was suggested to explain why sulfate reduction was not outcompeted by Fe reduction after the Fe oxide addition.

The aim of the present study was to investigate the microbiology of Mn and Fe reduction and the competitive relationships between these processes and sulfate reduction in coastal marine sediments. The investigations were performed on stations along a transect across the Black Sea shelf to the rim of the anoxic basin, where a range of bottom water oxygen concentrations potentially limit the cycling of Mn and Fe to various degrees. Furthermore, the sediments had moderately high Mn concentrations. We determined the rates of Mn, Fe, and sulfate reduction relative to the distribution of Mn and Fe oxides and analyzed the microbiology of Mn and Fe reduction.

#### MATERIALS AND METHODS

**Sites and sampling.** This study was conducted in September 1997 onboard RV *Petr Kottsov* on four stations on the Romanian Black Sea shelf (Fig. 1). The deepest station was located at the shelf break at a depth which, at the time of sampling, coincided with the oxic-anoxic interface in the water column (Table 1) (A. Weber, W. Riess, F. Wenzhöfer, and B. B. Jørgensen, submitted for publication). At all stations, the sediment was covered by an ~1-cm-thick layer of small shells of *Mytilus galloprovincialis* and *Modiolus phaseolinus* filled in with fine-grained sediment. At stations I to III, the mussels dominated the fauna,

while biomass decreased strongly from I to III (W. Riess, U. Luth, and F. Wenzhöfer, unpublished data). At station IV, only hydroids and meiofauna were observed. Below the shell layer, the sediments were fine-grained brown muds with a high shell content and few or no faunal burrows.

Sediment cores of 9.6 cm in diameter, up to 40 cm long, and visually undisturbed were retrieved with a multiple corer and immediately brought to a cold room at 8°C, where all subsequent handling for pore water analysis and incubations took place. Sediment for microbiological and molecular ecological analyses was subsampled and processed immediately after retrieval of cores.

**Sediment incubations.** For the determination of total anaerobic mineralization rates and the relative contributions of manganese, iron, and sulfate reduction, sediment from seven cores was sliced in 0.5- to 2-cm-thick sections to a depth of 10 cm, and parallel sections were pooled, mixed, and loaded into gastight plastic bags, all in an N<sub>2</sub>-filled glove bag as previously described (67). The bags of sediment were incubated in the dark at 8°C in larger N<sub>2</sub>-filled bags to ensure anoxia.

The dependence of microbial Fe reduction on the presence of Fe oxide was further investigated at station I, where the sediment from 0.5 to 1.5 cm and 8 to

TABLE 1. Sites of sediment sampling

Station	Water depth (m)	Sediment temp (°C)	Bottom water oxygen concn (μM)
I	62	6.6	211
II	77	7.2	213
III	100	7.6	75
IV	130	8	0

10 cm was split into two portions, one of which was amended with 40  $\mu\text{mol}$  of  $\text{Fe cm}^{-3}$  as 2-line ferrihydrite [ $\text{Fe}(\text{OH})_3$ ] from a 280-mmol-liter $^{-1}$   $\text{N}_2$ -purged suspension synthesized from  $\text{FeCl}_3$  (59).

Subsamples for pore water analysis were withdrawn five to six times during 2 weeks. In the glove bag, the sediment was loaded into centrifuge tubes leaving no headspace, and after centrifugation the supernatant was withdrawn and filtered through 0.45- $\mu\text{m}$ -pore-diameter cellulose acetate filters in an anoxic glove bag. A 1.8-ml aliquot was collected for  $\Sigma\text{CO}_2$  (total dissolved inorganic carbon) and  $\text{NH}_4^+$  analysis in glass vials with no headspace and stored at 4°C, ~2 ml were acidified with 6N HCl (1:100 vol) and stored at 4°C for  $\text{Mn}^{2+}$ ,  $\text{Fe}^{2+}$ , and  $\text{Ca}^{2+}$  determination, and an ~1-ml aliquot for  $\text{H}_2\text{S}$  and  $\text{SO}_4^{2-}$  analysis was preserved with 50- $\mu\text{l}$  of 2 M Zn acetate. Pore water pH was determined in whole sediment with a glass electrode calibrated with NBS buffers. Sediment for analysis of Mn and Fe in the solid phase was sampled at the beginning of the incubations and stored frozen. Sulfate reduction rates were determined by the radiotracer technique (25) three times during each incubation in subsamples of sediment loaded into cut off glass syringes. Reduced  $^{35}\text{S}$  was recovered in a single-step  $\text{Cr}^{2+}$  distillation, and sulfate reduction rates were calculated according to reference 22. The initial distribution of  $\text{NO}_3^-$  and  $\text{NO}_2^-$  at each station was determined in a separate sediment core, which was sectioned under  $\text{N}_2$  shortly after retrieval. Pore water was extruded as in the incubations, and a 2-ml aliquot for  $\text{NO}_3^- + \text{NO}_2^-$  analysis was stored frozen.

**Chemical analyses.** Pore water constituents were analyzed by the following procedures:  $\Sigma\text{CO}_2$  and  $\text{NH}_4^+$ , flow injection analysis with conductivity detection (23);  $\text{NO}_3^- + \text{NO}_2^-$ , chemiluminescence detection of NO produced by reduction with V(III) (8);  $\text{Mn}^{2+}$  and  $\text{Ca}^{2+}$ , flame atomic absorption spectrometry;  $\text{Fe}^{2+}$ , colorimetry with Ferrozine (62, 68);  $\text{H}_2\text{S}$ , colorimetry with methylene blue (14); and  $\text{SO}_4^{2-}$ , nonsuppressed anion chromatography.

Particulate Mn was quantified through extraction with dithionite-citrate-acetic acid (33). Poorly crystalline Fe(III) was determined by a combination of oxic and anoxic ammonium oxalate extractions (67). The extractions were made in duplicate.

**Calculations.** Accumulation rates of pore water constituents were calculated from slopes  $\pm$  standard errors of linear regression lines of concentrations versus time. Contrary to previous applications of the incubation technique,  $\Sigma\text{CO}_2$  concentrations were significantly affected by calcium carbonate precipitation (see Results). Rates of  $\text{CaCO}_3$  precipitation were calculated from changes in soluble  $\text{Ca}^{2+}$ , taking into account that these changes are partially compensated for by reversible sorption to particle surfaces (5):

$$\Delta\text{CaCO}_3 = \Delta[\text{Ca}^{2+}]_{\text{sol}}(1 + K_{\text{Ca}}) \quad (1)$$

where  $K_{\text{Ca}}$  is the adsorption constant for  $\text{Ca}^{2+}$  ( $K_{\text{Ca}} = 1.6$ ) (30). Rates of  $\Sigma\text{CO}_2$  production corrected for  $\text{CaCO}_3$  precipitation were calculated as

$$\Sigma\text{CO}_2 \text{ production} = \Sigma\text{CO}_2 \text{ accumulation} + \text{CaCO}_3 \text{ precipitation} \quad (2)$$

The saturation states of pore waters with respect to rhodocrocite ( $\text{MnCO}_3$ ) and siderite ( $\text{FeCO}_3$ ) were calculated by using PHREEQ-C with the thermodynamic constants of the PHREEQ database (50). Seawater compositions were calculated to the appropriate bottom water salinities (45) with the measured values of pH and concentrations of  $\text{Ca}^{2+}$ ,  $\Sigma\text{CO}_2$ ,  $\text{Mn}^{2+}$ , and  $\text{Fe}^{2+}$ .

**Enumeration of Mn and Fe reducers.** At all stations, acetate-oxidizing Mn- and Fe-reducing bacteria were enumerated by the MPN technique with acetate as the sole organic carbon source and either ferrihydrite or vernadite ( $\delta\text{MnO}_2$ ) as an electron acceptor. Sediment from a depth of 1 to 2 cm served as a primary inoculum. The anaerobic, sulfate-free, bicarbonate-buffered marine mineral medium with vitamins and trace elements (19, 71) was supplemented with 10 mM acetate and 40 mmol of either 2-line ferrihydrite or vernadite per liter (46). The MPN tube batteries were inoculated anaerobically in 10-fold dilution steps and incubated at 20°C for 1 year. Positive tubes were recognized from the change in the color of the precipitates from reddish brown to black (Fe) and from dark brown to white (Mn) (34). Results were calculated according to standard procedures (18).

**Molecular methods.** The natural microbial populations were analyzed at all stations by 4',6'-diamidino-2-phenylindole (DAPI) staining and fluorescent in situ hybridization (FISH) in sediment sectioned in 0.5-cm intervals, and the highest positive dilutions from the MPN series of stations I, II, and IV were analyzed by 16S rRNA gene amplification, cloning, and sequencing. Sample manipulation, fixation, and subsequent processing were performed as previously published (55). PCR amplification of the nearly complete 16S rRNA genes was performed with universal primers (24). New sequences were added to an alignment of about 13,000 homologous bacterial 16S rRNA primary structures (42; <http://www.mikro.biologie.tu-muenchen.de>) by using the aligning tool of the ARB program package (<http://www.mikro.biologie.tu-muenchen.de>). Distance matrix, maximum-parsimony, and maximum-likelihood methods were applied as implemented in the ARB software package. Phylogenetic trees were constructed by using subsets of data that included complete or almost complete sequences of representative members of *Proteobacteria*. Topologies were evaluated by using the different approaches to elaborate a consensus tree (41).

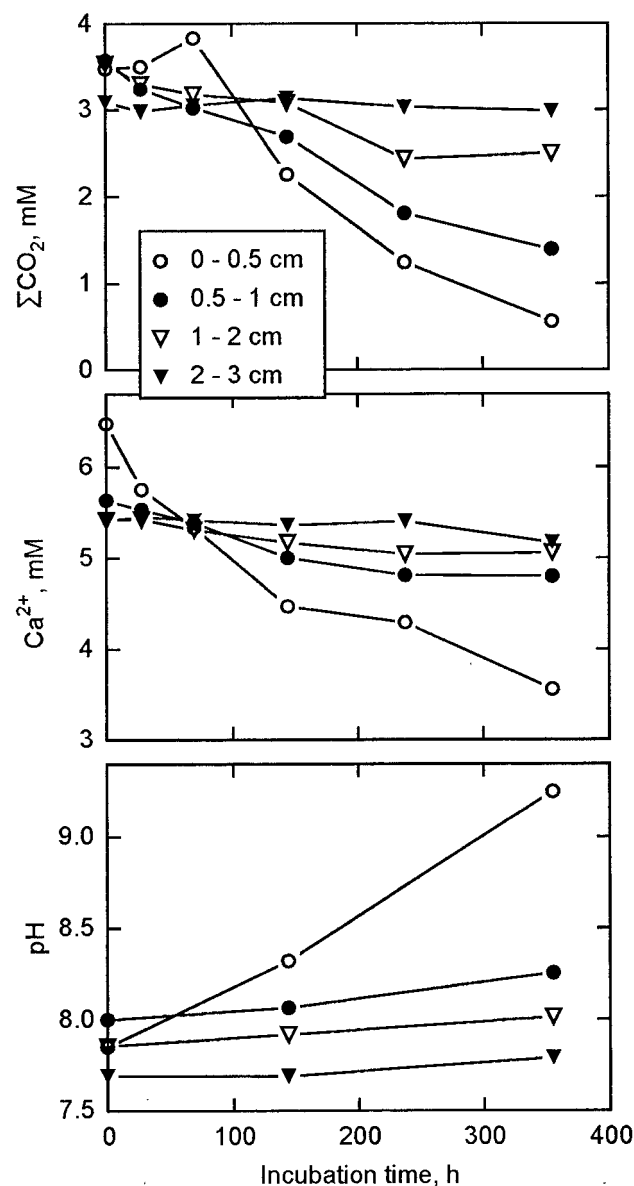
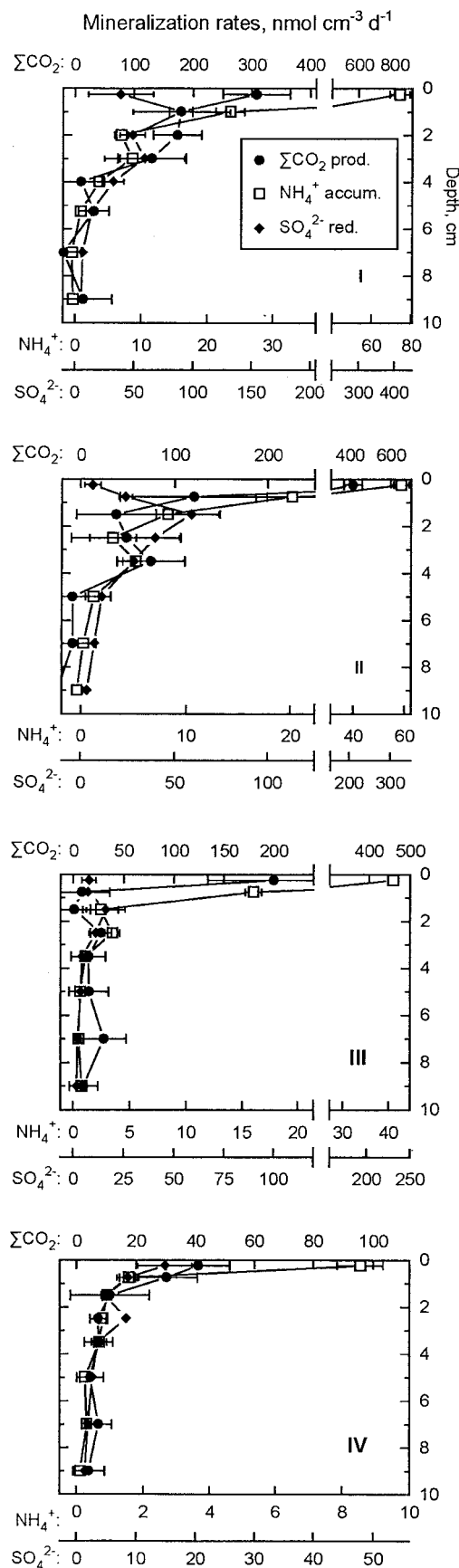


FIG. 2. Changes in the pore water constituents: total dissolved inorganic carbon ( $\Sigma\text{CO}_2$ ), calcium, and pH during anoxic incubation of the four upper depth intervals at station III.

## RESULTS

**$\Sigma\text{CO}_2$  production and carbonate precipitation.** At all four stations, the  $\Sigma\text{CO}_2$  concentration typically increased linearly throughout the incubation, and accumulation rates decreased toward zero with sediment depth (data not shown). The exceptions to this were all of the 0- to 0.5-cm intervals as well as the 0.5- to 2-cm intervals at station III, where  $\Sigma\text{CO}_2$  concentrations decreased significantly either from the beginning or after an initial rise (Fig. 2). The decreasing  $\Sigma\text{CO}_2$  concentrations were accompanied by decreasing concentrations of  $\text{Ca}^{2+}$  (Fig. 2), which demonstrated an involvement of  $\text{CaCO}_3$  precipitation. This precipitation was further associated with marked increases in pH at all stations, while no pH changes were detected in the deeper sediment sections (Fig. 2). Rates of  $\text{CaCO}_3$  precipitation (equation 1) in the surface sections were of similar magnitude to the initial  $\Sigma\text{CO}_2$  accumulation



rates. No precipitation was observed below a depth of 2 to 3 cm (data not shown).

When  $\text{CaCO}_3$  precipitation was included in the calculations of  $\Sigma\text{CO}_2$  production (equation 2), the highest production rates were observed in the 0- to 0.5-cm interval at all stations and decreased 10-fold from station I to station IV (Fig. 3). Rates also decreased strongly with depth in the sediment, and in the deeper sections,  $\Sigma\text{CO}_2$  production was hardly detectable.

In addition to  $\text{CaCO}_3$  precipitation,  $\Sigma\text{CO}_2$  may also have been affected by the precipitation of Mn carbonate, because pore waters were generally strongly supersaturated with rhodocrocite ( $\text{MnCO}_3$ ), with ion activity products exceeding the solubility constant more than fivefold to a depth of 2 cm at stations I to III. However, because  $\text{Mn}^{2+}$  was produced simultaneously by Mn reduction (see below), a correction of  $\Sigma\text{CO}_2$  production similar to the one made for  $\text{CaCO}_3$  was not possible (see also Discussion). Iron carbonate precipitation was not of general importance, because siderite ( $\text{FeCO}_3$ ) supersaturation only developed toward the end of the incubation at station I (0 to 2 cm) and station II (0.5 to 2 cm) (data not shown).

**$\text{NH}_4^+$  accumulation.** Similar to  $\Sigma\text{CO}_2$  production, the mineralization of organic nitrogen resulted in maxima of  $\text{NH}_4^+$  accumulation in the pore water at 0- to 0.5-cm depth at all sites with rates decreasing rapidly and approaching zero below 4 cm (Fig. 3). The rates decreased offshore, with an  $\sim 10$ -fold difference between maximum rates at stations I and IV, similar to the difference in  $\Sigma\text{CO}_2$  production.

**Nitrate reduction.** Nitrate and nitrite were not important as electron acceptors during the incubations, because only small peaks of  $\text{NO}_2^- + \text{NO}_3^-$  were initially located at 0 to 0.5 cm, with concentrations of 7, 11, 8, and 4  $\mu\text{M}$  at stations I through IV. Below 0.5 cm, initial concentrations were at a background level of  $\leq 2 \mu\text{M}$ .

**Mn and Fe reduction.** Extractable Mn was present in high concentrations ( $\geq 25 \mu\text{mol cm}^{-3}$ ) at 0 to 0.5 cm at all stations (Fig. 4). Manganese concentrations decreased with depth and reached stable levels below 1 to 2 cm, suggesting the depletion of reactive Mn oxides around this depth. At stations I to III, this depth distribution of reactive Mn oxide was further supported by the parallel distribution of accumulation rates of soluble  $\text{Mn}^{2+}$  (Fig. 4). At station IV, however,  $\text{Mn}^{2+}$  accumulation was restricted to a 0- to 0.5-cm depth, and since results concerning Fe and sulfate reduction at this site were also consistent with a depletion of reactive Mn below this interval, we interpret the elevated concentrations of extractable Mn at 0.5 to 2 cm as nonreactive Mn, possibly an authigenic Mn(II) phase. The maximum  $\text{Mn}^{2+}$  accumulation rates decreased offshore, but at all stations, rates corresponded to the accumulation of  $\geq 250 \mu\text{M Mn}^{2+}$ .

Concentrations of poorly crystalline Fe(III) were similar to those of Mn at the surface (excluding a particularly high Mn content at station II), but Fe(III) penetrated deeper into the sediment and first reached low background concentrations at a depth of  $\sim 3$  cm (Fig. 4). In contrast to the rapid accumulation of  $\text{Mn}^{2+}$ , soluble  $\text{Fe}^{2+}$  concentrations generally increased by

FIG. 3. Vertical profiles of organic matter mineralization rates in Black Sea sediments from station I (top) to station IV (bottom). Circles,  $\Sigma\text{CO}_2$  production; squares,  $\text{NH}_4^+$  accumulation; diamonds, sulfate reduction. Error bars indicate standard errors from linear regressions ( $\Sigma\text{CO}_2$  and  $\text{NH}_4^+$ ) and standard deviations of triplicate sulfate reduction rates. Note different scales for different processes. At each station, the three scales are plotted at the ratio 11.2:1:5.6 for  $\Sigma\text{CO}_2$  production/ $\text{NH}_4^+$  accumulation/sulfate reduction, corresponding to the inferred stoichiometric ratio of these processes during sulfate reduction (see text for details).

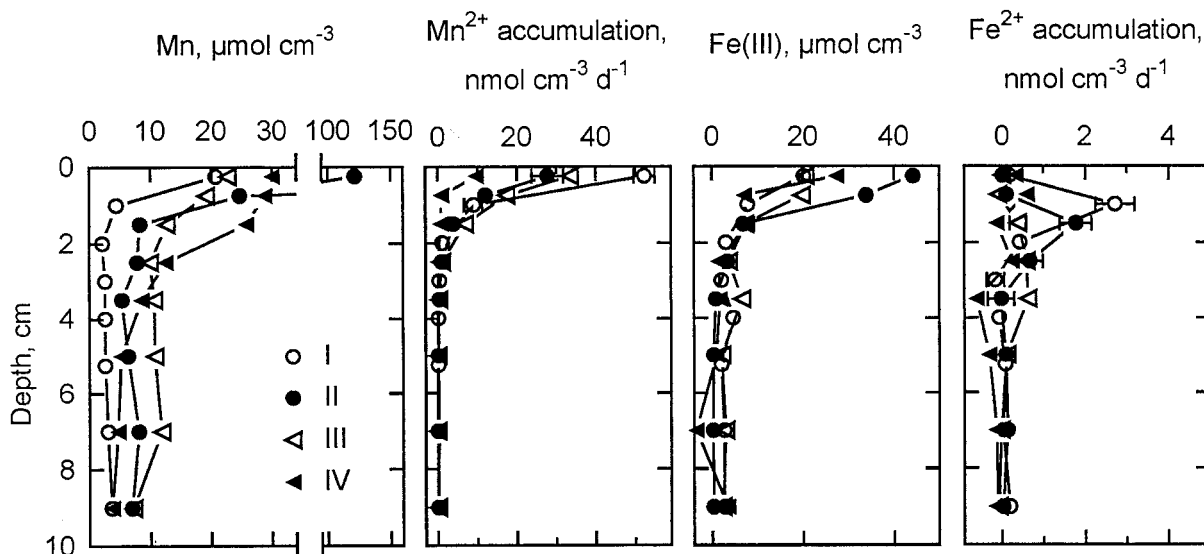


FIG. 4. Depth distributions at stations I to IV of (left to right) extractable Mn,  $\text{Mn}^{2+}$  accumulation rates during anoxic incubations, poorly crystalline Fe(III), and  $\text{Fe}^{2+}$  accumulation rates. Concentrations are means of duplicate determinations, and error bars indicate standard errors of rates.

$\leq 10 \mu\text{M}$  during the 2 weeks, with small peaks of accumulation located below the peak of  $\text{Mn}^{2+}$  accumulation at each station (Fig. 4). As was the case for  $\text{Mn}^{2+}$ , the rates were highest at station I.

**Sulfate reduction rates.** At stations I to III, sulfate reduction rates increased from the surface to a maximum at a depth of 1 to 2 cm, below which rates decreased asymptotically toward zero (Fig. 3). At station IV, the rate was highest in the surface 0 to 0.5 cm. Both maximum and integrated rates decreased approximately fivefold offshore along the transect.

Bottom water sulfate concentrations were 14 to 17 mM and the decrease in pore-water concentration over the upper 10 cm at all sites was  $\leq 2$  mM. At all stations and depths, the initial concentration of  $\text{H}_2\text{S}$  was  $< 1 \mu\text{M}$ , but slight accumulations to  $\leq 10 \mu\text{M}$  were observed below a depth of 3 cm at all stations during the first 2 weeks of incubation, with the highest rates at station IV (data not shown).

Assuming an overall stoichiometry of 2 mol of organic carbon to 1 mol of sulfate for carbon oxidation, with sulfate as the terminal electron acceptor (67), there was a good agreement between sulfate reduction-based and measured  $\Sigma\text{CO}_2$  production rates below  $\sim 1$  cm of depth at all stations, implying that all  $\Sigma\text{CO}_2$  production there could be attributed to sulfate reduc-

tion. In contrast, the measured  $\Sigma\text{CO}_2$  production at the surface significantly exceeded that calculated from sulfate reduction rates at stations I to III, while at station IV, only a small excess  $\Sigma\text{CO}_2$  production was indicated.

Sulfate reduction and ammonium accumulation rates were also closely correlated below 1 cm of depth at all sites ( $r^2 = 0.87$ ) with a ratio of sulfate reduction to ammonium accumulation for all stations of  $5.6 \pm 0.4:1$ , which corresponds to a ratio of carbon oxidation to ammonium accumulation of ( $2 \cdot 5.6 =$ ) 11.2:1.

**Addition of ferrihydrite.** In the sediment from depths of both 0.5 to 1.5 and 8 to 10 cm at station I amended with ferrihydrite, soluble  $\text{Fe}^{2+}$  accumulated at rates two to three times higher than in the unamended controls, while  $\text{H}_2\text{S}$  remained undetectable. However, addition of ferrihydrite had no significant effect on either sulfate reduction rates,  $\Sigma\text{CO}_2$  production, or ammonium accumulation (Student's  $t$  test;  $P > 0.05$ ) (Table 2).

**Bacterial counts.** At all four stations, total bacterial counts were highest at the surface and decreased exponentially with depth, and cell numbers reached  $\sim 10\%$  of the surface value at 10 cm (data not shown; see profile from station II in reference 55). Cell numbers decreased slightly offshore, with maxima of  $3.6 \times 10^9$ ,  $2.0 \times 10^9$ ,  $1.7 \times 10^9$ , and  $0.9 \times 10^9$  cells  $\text{cm}^{-3}$  at stations I through IV. The 1- to 2-cm layers used for MPN enumerations held numbers close to these maxima:  $2.2 \times 10^9$ ,  $1.5 \times 10^9$ ,  $1.5 \times 10^9$ , and  $0.5 \times 10^9$  cells  $\text{cm}^{-3}$  at stations I through IV. Detection rates as well as single-cell signal intensities with FISH using the general probe for bacteria EUB338 (4) were very low in all sediments. The rates were  $\leq 20\%$  of total cell counts at stations I to III and  $\leq 4\%$  at station IV in the layer where MPN counts were performed. At all stations, the fraction of total cells that were detected with FISH decreased with depth, and the decreases through the vertical profile were parallel to the decreases in  $\Sigma\text{CO}_2$  production and  $\text{NH}_4^+$  accumulation rates (see also reference 55).

The MPN counts resulted in extremely low numbers of Fe-reducing acetate oxidizers, since Fe reduction only occurred at the lowest dilution (Table 3). In contrast, the MPNs of Mn reducers were up to  $1.1 \times 10^5$  cells  $\text{cm}^{-3}$  with this maximum at

TABLE 2. Effects of ferrihydrite amendments on mineralization rates at station I

Process	Treatment	Mineralization rate (nmol $\text{cm}^{-3} \text{ day}^{-1}$ ) at depth <sup>a</sup> :	
		0.5–1.5 cm	8–10 cm
$\Sigma\text{CO}_2$ production	Unamended	$179 \pm 20$	$14 \pm 49$
	+ Ferrihydrite	$200 \pm 67$	$71 \pm 24$
$\text{NH}_4^+$ accumulation	Unamended	$24 \pm 2$	$-0.3 \pm 0.2$
	+ Ferrihydrite	$26 \pm 4$	$-0.2 \pm 0.6$
Sulfate reduction	Unamended	$97 \pm 23$	$5.2 \pm 0.9$
	+ Ferrihydrite	$109 \pm 42$	$3.4 \pm 0.3$

<sup>a</sup> Values are means  $\pm$  standard errors.

TABLE 3. MPN counts of acetate-oxidizing, Mn- and Fe-reducing bacteria in Black Sea sediments

Station	Mn reducers		Iron reducers	
	MPN (cells cm <sup>-3</sup> )	95% Confidence interval	MPN (cells cm <sup>-3</sup> )	95% Confidence interval
I	2.1 × 10 <sup>3</sup>	350–4.7 × 10 <sup>3</sup>	23	4–120
II	1.1 × 10 <sup>5</sup>	1.5 × 10 <sup>4</sup> –4.8 × 10 <sup>5</sup>	23	4–120
III	1.1 × 10 <sup>3</sup>	150–4.8 × 10 <sup>3</sup>	23	4–120
IV	460	71–2.4 × 10 <sup>3</sup>	23	4–120

station II and the minimum at station IV (Table 3). The complete reduction of 40 mmol MnO<sub>2</sub> liter<sup>-1</sup> in the MPN tubes indicated that the oxidation of all of the 10 mM acetate added was coupled to Mn reduction.

**Molecular screening.** From the highest positive MPN dilutions with MnO<sub>2</sub> at stations I, II, and IV, rRNA genes were amplified and cloned after 3 months of incubation. Fifteen clones from each library were screened with ARDRA (53) to distinguish different restriction patterns that were then sequenced. This resulted in two clone types from station I (A3Mn1 and A3Mn2) and only one clone type each from stations II and IV (B4Mn1 and D1Mn1). The 16S rRNA phylogenetic reconstruction showed that the clones A3Mn1, B4Mn1, and D1Mn1 were affiliated with the branch that comprises the genus *Arcobacter* in the  $\epsilon$ -subclass of Proteobacteria (Fig. 5). Two clone types, A3Mn1 and B4Mn1, were nearly identical. The second most abundant organism from station I was affiliated with *Desulfuromonas acetoxidans* and *Pelobacter* species.

Attempts to continue the cultures from the highest positive dilutions with acetate were unsuccessful. Subcultivation of the MPN culture from the lowest dilution at station IV on lactate and  $\delta$ MnO<sub>2</sub> resulted in the enrichment of an organism, strain D1Mn, which was isolated and identified as belonging to the genus *Shewanella*. Phylogenetic analysis of the rRNA sequence showed that its closest known relatives were *Shewanella* species isolated from Antarctic sea ice (Fig. 5).

## DISCUSSION

No method is currently available for a direct quantification of organotrophic microbial Mn and Fe reduction rates in natural environments such as marine sediments, where reduced inorganic species will compete with organic matter as reductants of the metal oxides (66). Instead, our approach was to identify zones in the sediment where carbon oxidation rates exceeded the carbon oxidation coupled to bacterial sulfate reduction and to assign the excess carbon oxidation to alternative dissimilatory processes according to the zonation of the electron acceptors O<sub>2</sub>, NO<sub>3</sub><sup>-</sup>, and Mn and Fe oxides. The principles of this method are discussed by Thamdrup and Canfield (66).

**Carbon oxidation and sulfate reduction.** A clear divergence of total and sulfate-based  $\Sigma$ CO<sub>2</sub> production rates demonstrated the importance of electron acceptors other than sulfate in the surface layers at stations I to III, whereas deeper in the sediment, and at all depths at station IV, contributions from other oxidants could not be discerned by this approach (Fig. 3). The complete dominance of sulfate reduction below depths of 1 to 2 cm at all stations was also supported by the stable background levels of metal oxides attained around a depth of

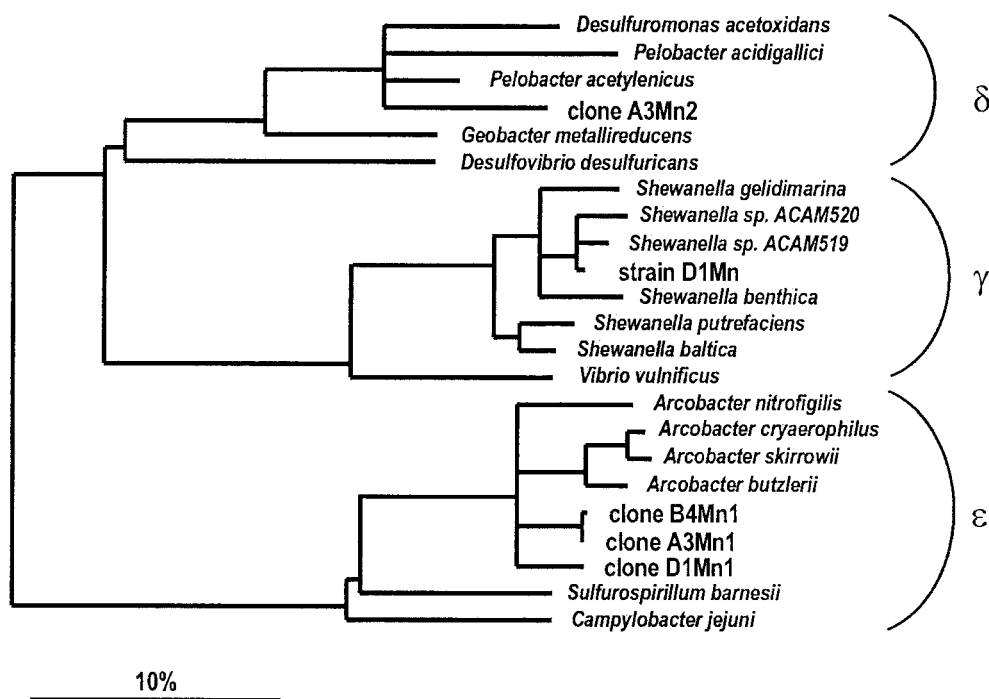


FIG. 5. 16S rRNA-based tree reflecting the phylogenetic relationships of the clone sequences and a selection of sequences belonging to different subclasses of Proteobacteria. The tree is based on the results of a maximum parsimony analysis including complete or almost complete 16S rRNA sequences from representative bacteria of a phylogenetic branch. The topology of the tree was evaluated and corrected according to the results of distance matrix, maximum parsimony, and maximum likelihood analyses of various data sets. Branching patterns within each subclass were also evaluated by using a 50% conservation filter for the members of their corresponding subclass (41). Multifurcations indicate topologies that could not be unambiguously resolved. The bar indicates 10% estimated sequence divergence. EMBL accession numbers of the new sequences are as follows: A3Mn2, AJ271656; D1Mn, AJ271657; B4Mn1, AJ271653; A3Mn1, AJ271655; and D1Mn1, AJ271654.

TABLE 4. Rates of carbon oxidation coupled to sulfate reduction and reduction of other electron acceptors during anoxic incubations of Black Sea sediments<sup>a</sup>

Station	Rate of C oxidation					Interval (cm) <sup>c</sup>
	Sulfate (mmol of C m <sup>-2</sup> day <sup>-1</sup> )	Other electron acceptor				
		ΣCO <sub>2</sub> production		NH <sub>4</sub> <sup>+</sup> accumulation		
		mmol of C m <sup>-2</sup> day <sup>-1</sup>	% <sup>b</sup>	mmol of C m <sup>-2</sup> day <sup>-1</sup>	% <sup>b</sup>	
I	5.68 ± 0.57	1.90 ± 1.05	25	4.41 ± 0.98	44	0–2.5
II	3.70 ± 0.22	2.39 ± 0.46	39	4.11 ± 0.26	53	0–1
III	1.10 ± 0.12	0.89 ± 0.36	45	3.04 ± 0.06	73	0–1
IV	0.81 ± 0.03	0.12 ± 0.09	13	0.34 ± 0.20	29	0–2

<sup>a</sup> Rates are expressed as means ± standard deviations for 0- to 10-cm sediment depth (see text for details of calculation).

<sup>b</sup> Percentage of total carbon oxidation during incubations.

<sup>c</sup> Depth interval used for calculation of non-sulfate-based carbon oxidation rates.

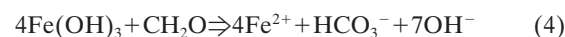
2 cm (Fig. 4). Accumulation of H<sub>2</sub>S in the deeper sections during the incubations further documented the absence of easily reducible metal oxides, since such oxides would rapidly scavenge H<sub>2</sub>S to submicromolar concentrations (12). Sulfate was also the single most important terminal electron acceptor when mineralization was stimulated by the addition of labile organic matter to sediment from a depth of 1 to 6 cm at station II (55).

The excess ΣCO<sub>2</sub> production in the surface sections of stations I to III corresponded to rates of 0.9 to 2.4 mmol m<sup>-2</sup> day<sup>-1</sup> or 33 to 81% of the carbon oxidation coupled to sulfate reduction (Table 4). However, the determination of ΣCO<sub>2</sub> production rates was complicated by carbonate precipitation, and although ΣCO<sub>2</sub> production rates were corrected for the precipitation of CaCO<sub>3</sub>, the strong supersaturation indicated that precipitation of MnCO<sub>3</sub> was also likely taking place. As will be discussed below, the carbonate precipitation was driven by the reduction of Mn and possibly Fe. It was therefore not possible to make corrections for the precipitation of carbonate with Mn<sup>2+</sup> or Fe<sup>2+</sup>, such as for Ca<sup>2+</sup>, and the ΣCO<sub>2</sub> production rates in the zones of Mn and Fe reduction are therefore minimum estimates of carbon oxidation rates.

Rates of ammonium accumulation provide an alternative estimate of the mineralization rates of organic matter in the zone of carbonate precipitation (13). In incubations similar to ours, with sediments free of carbonate precipitation, good correlations have been found between rates of carbon mineralization and NH<sub>4</sub><sup>+</sup> accumulation (13, 26, 27, 67). In the subsurface layers of the Black Sea sediments, where sulfate reduction was the only significant respiratory pathway, there was also a close correlation between rates of sulfate reduction and NH<sub>4</sub><sup>+</sup> accumulation with a ratio of sulfate-based carbon oxidation to NH<sub>4</sub><sup>+</sup> accumulation of 11.2:1 for all stations, which is in good agreement with such ratios observed in other sediments with low activity (13, 26, 27, 67). The sulfate reduction rates are preferred for the determination of an NH<sub>4</sub><sup>+</sup>/ΣCO<sub>2</sub> production ratio over a direct correlation of NH<sub>4</sub><sup>+</sup> and ΣCO<sub>2</sub> production rates because of the smaller coefficients of variance associated with sulfate reduction than with ΣCO<sub>2</sub> production determinations (Fig. 3). In Fig. 3, the scales for ΣCO<sub>2</sub> production and NH<sub>4</sub><sup>+</sup> accumulation are plotted at a ratio of 11.2:1. Thus, ΣCO<sub>2</sub> production rates estimated from this ratio and NH<sub>4</sub><sup>+</sup> accumulation rates can be found by projection of the data points for NH<sub>4</sub><sup>+</sup> accumulation onto the ΣCO<sub>2</sub> production axis.

The NH<sub>4</sub><sup>+</sup>-based estimates confirm the small contribution of sulfate reduction to mineralization in the upper sections at all stations. Furthermore, the rates of ΣCO<sub>2</sub> production calculated from NH<sub>4</sub><sup>+</sup> data are up to threefold higher than the measured rates of ΣCO<sub>2</sub> production near the sediment surface (Table 4), which suggests that a large part of the produced ΣCO<sub>2</sub> precipitated immediately with Mn<sup>2+</sup> (or Fe<sup>2+</sup> at stations I and II) and implies a greater importance of electron acceptors other than sulfate than calculated from the direct determinations of ΣCO<sub>2</sub> production (Table 4). The NH<sub>4</sub><sup>+</sup>-based rates can be considered as upper limits of the actual rates. This is because the steep increases in mineralization rates toward the surface could be associated with a moderate decrease in ΣCO<sub>2</sub>/NH<sub>4</sub><sup>+</sup> production ratios (27, 28, 67).

**Mn and Fe reduction.** The depth distribution of electron acceptors implied that the non-sulfate-based carbon oxidation in the incubations was coupled to the reduction of Mn or Fe oxides. The increases in pH with time, which correlated with the rates of excess carbon oxidation, were also consistent with Mn or Fe reduction as terminal electron-accepting processes, whereas only small pH changes are expected during sulfate reduction (11):



Mn reduction was directly evidenced by the rapid accumulation of soluble Mn<sup>2+</sup>, the rates and depth distribution of which correlated well with the rates of excess carbon oxidation (Fig. 3 and 4). In contrast, changes in soluble Fe<sup>2+</sup> concentrations gave no strong indications of Fe reduction. Although zones of microbial Mn and Fe reduction in sediments are often indicated by the accumulation of Mn<sup>2+</sup> and Fe<sup>2+</sup>, the pore water accumulation rates are typically lower than the gross production rates of Mn(II) and Fe(II) by an order of magnitude or more due to adsorption and/or precipitation (9, 13, 60). The ratio of the rates of excess ΣCO<sub>2</sub> production (NH<sub>4</sub><sup>+</sup>-based) to Mn<sup>2+</sup> accumulation in the present study (~1:15; compare Fig. 3 and 4) was consistent with the range of sorption coefficients determined for Mn-rich sediment (13). Thus, it is feasible that the excess carbon oxidation was coupled to Mn reduction.

Little is known about the modes of Fe(II) sorption in sediments, and Fe reduction cannot be excluded based on the low rates of Fe<sup>2+</sup> accumulation. Furthermore, Fe reduction in the presence of Mn oxides is masked by rapid abiotic reoxidation (38, 47, 51). Two other lines of evidence suggest, however, that dissimilatory microbial Fe reduction did not play a significant role in carbon oxidation in the Black Sea sediments: (i) MPN counts showed very low numbers of Fe-reducing bacteria (FeRB) at the depth in the sediment where the process could be important (Table 3), and (ii) addition of ferrihydrite had no discernible effect on the pathways of carbon oxidation (Table 2).

The MPN counts of FeRB (~10 cm<sup>-3</sup>; Table 3) were low both compared to total bacterial counts, which were similar to counts in other fine-grained continental marine sediments (~10<sup>9</sup> cm<sup>-3</sup>) (57, 58), to the counts of Mn-reducing bacteria (10<sup>3</sup> to 10<sup>5</sup> cm<sup>-3</sup>) in the same sediment, and to the relatively few other MPN enumerations of acetate-utilizing FeRB reported from other marine sediments (10<sup>3</sup> to 10<sup>7</sup> cm<sup>-3</sup>) (15, 19). Thus, although viable counts are likely to underestimate the size of the total FeRB community, the relative abundances imply poor growth conditions for FeRB in the Black Sea sediments.

In the marine sediments investigated so far, the contribution of dissimilatory Fe reduction to carbon oxidation has been found to be limited by Fe(III) at in situ concentrations of poorly crystalline Fe(III) below  $30 \mu\text{mol Fe(III) cm}^{-3}$  (65). Thus, below a depth of 0.5 to 1 cm in the Black Sea sediments, dissimilatory Fe reduction is predicted to be strongly inhibited by the low Fe(III) concentrations (Fig. 4). The competitive relationship between microbial Fe and sulfate reduction is presumed to function through concentrations of important common substrates such as acetate and  $\text{H}_2$ , where Fe reduction may deplete these concentrations below the threshold of utilization by sulfate reduction when sufficient Fe(III) is available (36, 37). Hence, if a significant population of FeRB were present, addition of ferrihydrite would be expected to relieve any inhibition of Fe reduction and allow this process to out-compete sulfate reduction, as previously demonstrated with estuarine and freshwater sediments (1, 37). The lack of response to the ferrihydrite additions therefore further supports that FeRB were not important. An analogous conclusion based on similar results has been reached for a marine sediment from San Diego Bay (15).

Manganese-reducing bacteria (MnRB) were counted in much higher numbers than FeRB, and there was a positive correlation between the rates of non-sulfate-based carbon oxidation and the numbers of MnRB. Furthermore, Mn oxide concentrations were as high as those of poorly crystalline Fe(III). Based on these results as well as the geochemical evidence for Mn reduction and the lack of biogeochemical and microbiological evidence for dissimilatory Fe reduction discussed above, we conclude that dissimilatory Mn reduction was responsible for the non-sulfate-based carbon oxidation during the incubations.

**Ecological significance of Mn reduction.** Based on a comparison of sulfate reduction rates measured in situ at the sea floor and in sediment cores onboard the ship during the cruise at the same stations as investigated here, it was concluded that the recovery of the sediment did not substantially affect sulfate reduction rates (Weber et al., submitted). Sulfate reduction rates in our incubations were quite similar to the rates determined in intact cores both in terms of maxima and depth distributions. We therefore expect that the total carbon mineralization rates from our incubations also provide good estimates of the in situ rates.

The contributions from dissimilatory Mn reduction (Table 4) were estimated from anoxic conditions. This corresponded to the conditions in situ at station IV, where the bottom water was anoxic at the time of sampling, and, consequently, the 13 to 29% contribution from dissimilatory Mn reduction estimated there should reflect the partitioning in situ. At the other stations with oxic bottom water, rates of dissimilatory Mn reduction in situ would have been smaller than in the incubations due to competition with organotrophic oxygen respiration. Due to the high shell content, it was not possible to directly determine the oxygen penetration depth in the sediments, but oxygen penetration depths ( $z_{\text{max}}$ ) can be estimated from the diffusive oxygen uptakes (DOU) of the sediments as determined from the oxygen microgradients just above the sediment surface (Weber et al., submitted) according to reference 6:

$$z_{\text{max}} = 2 C_o D_s \phi / \text{DOU} \quad (6)$$

where  $C_o$  is the concentration at the sediment surface,  $D_s$  is the sediment diffusion coefficient of  $\text{O}_2$ , and  $\phi$  is porosity (see also reference 52). Estimates of  $z_{\text{max}}$  from DOU for stations I, II, and III, respectively, are 1.5, 4.6, and 3.3 mm. Hence, oxygen is predicted to be present in situ in only a part of the

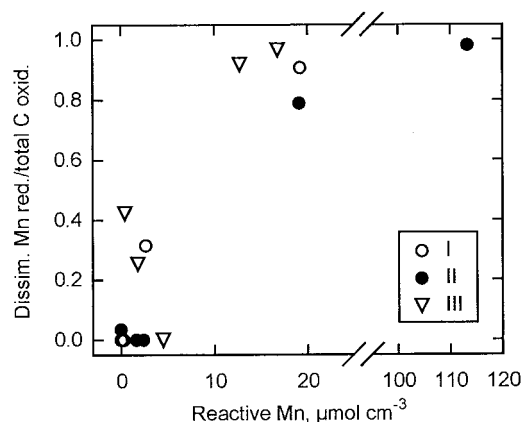


FIG. 6. The relative contribution of dissimilatory Mn reduction to carbon oxidation as a function of the reactive Mn concentration in sediment from individual depth intervals from stations I to III in the Black Sea. Reactive Mn was calculated by subtraction of the average background concentration at a 4- to 10-cm depth from each station (see text for references).

depth intervals where non-sulfate-based carbon oxidation occurred. The competitive relationship between Mn and oxygen respiration is not well explored, and we can therefore not further constrain the relative importances of the two processes in situ.

The turnover of Mn oxide in coastal sediments is relatively fast, and maintenance of Mn reduction requires efficient recycling of  $\text{Mn}^{2+}$  by reoxidation with oxygen (3, 68). Along the transect, carbon oxidation rates and bottom water oxygen concentrations varied in parallel (Tables 1 and 4), and it appears that a balance in Mn oxide demand and reoxidation potential leads to roughly similar relative contributions of Mn reduction at all sites. Significant Mn reduction cannot be maintained at station IV in the absence of oxygen. However, ~25-m fluctuations in the depth of the chemocline were observed during the two-week cruise (B. B. Jørgensen and A. Weber, personal communication), which would allow oxygen to reach the sediment at station IV periodically. Fluctuating bottom water oxygen concentrations at the outer shelf stations may thus cause large temporal variations in the rates of microbial Mn reduction.

Significant contributions from dissimilatory Mn reduction to benthic carbon oxidation have only been demonstrated in two earlier cases (2, 10). Both of these were from well-ventilated offshore basins with extreme concentrations of Mn oxides ( $\geq 100 \mu\text{mol cm}^{-3}$ ), i.e., environments much different from the Black Sea sediments. In our incubations, the relative contribution of dissimilatory Mn reduction to carbon oxidation depended on the concentration of reactive Mn, with strong inhibition of sulfate reduction at concentrations above  $\sim 10 \mu\text{mol cm}^{-3}$  (Fig. 6). The reactive Mn concentrations in Fig. 6 were calculated by subtraction of the low unreactive background concentrations measured at depths of 4 to 10 cm at each site (3) (Fig. 4). Station IV was excluded from these calculations because of the high concentrations of nonreactive Mn measured at 0.5 to 2 cm. A similar relationship to that in Fig. 6 has been observed and discussed for the competition between iron and sulfate reduction in marine sediments (65).

Coastal marine sediments have typical maximum concentrations of reactive Mn of  $< 10 \mu\text{mol cm}^{-3}$  restricted to the upper millimeters, and the relationship in Fig. 6 predicts that dissimilatory Mn reduction is of little importance in such sediments, thus supporting previous conclusions (3, 13, 56, 67, 68). Higher



Mn concentrations, as found in the Black Sea, are observed in sediments in coastal troughs and bordering low-oxygen basins (49, 63), and consequently, dissimilatory Mn reduction may be of importance there. Although dissimilatory Mn reduction is not of general importance in marine sediments, the present results indicate that the process may be found in considerably wider areas than previously recognized.

**Mn- and Fe-reducing bacteria.** Most known dissimilatory Fe-reducing bacteria also reduce Mn oxide when tested (35, 65), and likewise, most organisms isolated as dissimilatory Mn reducers also grow with Fe(III) as the electron acceptor (7, 20, 29). It was therefore a surprise to find much higher numbers of MnRB than FeRB in otherwise identical MPN series. Because the cultures could not be continued, we have no definite proof that the MnRB could not utilize Fe(III), but they must reduce Mn oxide much more efficiently than ferrihydrite. This suggests that Mn reduction is not necessarily conveyed by Fe reducers and that organisms that specialized in Mn reduction could play a relevant role in environments with abundant Mn oxide. The clone-type A3Mn2 from station I was affiliated with the *Desulfuromonas-Pelobacter* cluster which contains numerous Fe-reducing bacterial species (16, 32). However, several of the species most closely related to the clone-type A3Mn2 from station I have been found to reduce only soluble Fe(III) complexes and not ferrihydrite (21, 32). The Mn-reducing capabilities of these organisms have not been reported.

The only Mn reducer that we could isolate was affiliated with the *Shewanella* branch of the  $\gamma$ -subclass of *Proteobacteria*. This strain, D1Mn, was obtained by subcultivation on lactate of an inoculum from the same MPN tube from which the clone library of station IV was established. However, no clones with identical or similar sequence were obtained in this library. High numbers of *Shewanella* cells have been found in the chemocline of the central Black Sea (48); however, in spite of its isolation, we do not have any clue about *Shewanella*'s environmental relevance as an Mn reducer in the sediment.

The exclusive recovery of *Arcobacter*-related organisms in the clone libraries from the highest positive dilutions of the MnRB MPN series at stations II and IV and their presence at station I are strong indications that these bacteria conducted the oxidation of acetate with Mn oxide in those series and that they were quantitatively significant in the Black Sea sediments. Dissimilatory Mn or Fe reduction has not been demonstrated for species of *Arcobacter* that are known as microaerophiles and nitrate reducers (64, 69). The only Mn- and Fe-reducing organism from the  $\epsilon$ -subclass of *Proteobacteria* yet in culture is *Sulfurospirillum barnesii* (29, 61). Thus, *Arcobacter*-related organisms may represent an ecologically significant new group of dissimilatory Mn-reducing bacteria. *Arcobacters* are mainly known as potential pathogens isolated from humans and livestock (69), but strains have also been isolated from salt marsh sediment and a hypersaline microbial mat (43, 44, 64). In further support of their ecological significance, species of *Arcobacter* have recently been detected by FISH in a marine tidal flat sediment, where they were most abundant ( $>10^7$  cm $^{-3}$ ) at depths of 0.5 to 2 cm (31). Their ecological role was not identified, but their concentration in the upper part of the anoxic sediment is in agreement with the depth distribution expected for an organism that grows by the reduction of Mn oxides.

Our results provide the first evidence that microbial Mn reduction may be important in carbon oxidation in shelf sediments. The relative contribution of Mn reduction to carbon oxidation depends on the Mn oxide concentration, which may thus be used as an indicator of sites where the process is potentially significant. Due to the rapid turnover and shallow

extension of Mn oxides, reduction rates are likely to vary temporally, e.g., in response to changes in bottom water oxygen concentrations. Large temporal and spatial variability is a general feature of the coastal Mn cycle (3, 68).

The integration of microbiological and biogeochemical approaches proved very useful for investigating the ecology of microbial Mn reduction, and the finding that Mn reduction was catalyzed by bacteria which were not previously known as Mn reducers emphasizes the need for a specific search for Mn-reducing microorganisms in the environment.

#### ACKNOWLEDGMENTS

We are grateful to Swantje Fleischer for skillful technical assistance and to Jan Kuever, Ingrid Kunze, and Karsten Zengler for help with MPN enumerations. We thank Andreas Weber and Bo Barker Jørgensen for excellent planning and coordination of the Black Sea cruise and the master, crew, and scientific party on R/V *Petr Kottsov* for a highly productive cruise.

This study was supported by the Max Planck Society and by the Danish Research Foundation through the Danish Center for Earth System Science.

#### REFERENCES

- Acht nich, C., F. Bak, and R. Conrad. 1995. Competition for electron donors among nitrate reducers, ferric iron reducers, sulfate reducers, and methanogens in anoxic paddy soil. *Biol. Fertil. Soils* **19**:65–72.
- Aller, R. C. 1990. Bioturbation and manganese cycling in hemipelagic sediments. *Phil. Trans. R. Soc. Lond.* **A331**:51–58.
- Aller, R. C. 1994. The sedimentary Mn cycle in Long Island Sound: its role as intermediate oxidant and the influence of bioturbation, O<sub>2</sub> and C<sub>org</sub> flux on diagenetic reaction balance. *J. Mar. Res.* **52**:259–295.
- Amann, R. L., B. J. Binder, R. J. Olson, S. W. Chisholm, R. Devereux, and D. A. Stahl. 1990. Combination of 16S rRNA-targeted oligonucleotide probes with flow cytometry for analyzing mixed microbial populations. *Appl. Environ. Microbiol.* **56**:1919–1925.
- Berner, R. A. 1980. *Early diagenesis*. Princeton University Press, Princeton, N.J.
- Bouldin, D. R. 1968. Models for describing the diffusion of oxygen and other mobile constituents across the mud-water interface. *J. Ecol.* **55**:77–87.
- Bowman, J. P., S. A. McCammon, D. S. Nichols, J. H. Skerratt, S. M. Rea, P. D. Nichols, and T. A. McMeekin. 1997. *Shewanella gelidimarina* sp. nov. and *Shewanella frigidimarina* sp. nov., novel Antarctic species with the ability to produce eicosapentaenoic acid (20:5 $\omega$ 3) and grow anaerobically by dissimilatory Fe(III) reduction. *Int. J. Syst. Bacteriol.* **47**:1040–1047.
- Braman, R. S., and S. A. Hendrix. 1989. Nanogram nitrite and nitrate determination in environmental and biological materials by vanadium(III) reduction with chemiluminescence detection. *Anal. Chem.* **61**:2715–2718.
- Canfield, D. E. 1993. Organic matter oxidation in marine sediments, p. 333–363. *In* R. Wollast, F. T. Mackenzie, and L. Chou (ed.), *Interactions of C, N, P, and S biogeochemical cycles and global change*. Springer, Berlin, Germany.
- Canfield, D. E., B. B. Jørgensen, H. Fossing, R. Glud, J. Gundersen, N. B. Ramsing, B. Thamdrup, J. W. Hansen, L. P. Nielsen, and P. O. J. Hall. 1993. Pathways of organic carbon oxidation in three continental margin sediments. *Mar. Geol.* **113**:27–40.
- Canfield, D. E., and R. Raiswell. 1991. Carbonate precipitation and dissolution, its relevance to fossil preservation, p. 411–453. *In* P. A. Allison and D. E. G. Briggs (ed.), *Taphonomy: releasing the data locked in the fossil record*. Plenum Press, New York, N.Y.
- Canfield, D. E., R. Raiswell, and S. Bottrell. 1992. The reactivity of sedimentary iron minerals toward sulfide. *Am. J. Sci.* **292**:659–683.
- Canfield, D. E., B. Thamdrup, and J. W. Hansen. 1993. The anaerobic degradation of organic matter in Danish coastal sediments: Fe reduction, Mn reduction and sulfate reduction. *Geochim. Cosmochim. Acta* **57**:2563–2570.
- Cline, J. D. 1969. Spectrophotometric determination of hydrogen sulfide in natural waters. *Limnol. Oceanogr.* **14**:454–458.
- Coates, J. D., R. T. Anderson, J. C. Woodward, E. J. P. Phillips, and D. R. Lovley. 1996. Anaerobic hydrocarbon degradation in petroleum-contaminated harbor sediments under sulfate-reducing and artificially imposed iron-reducing conditions. *Environ. Sci. Technol.* **30**:2784–2789.
- Coates, J. D., D. J. Lonergan, E. J. P. Phillips, H. Jenter, and D. R. Lovley. 1995. *Desulfuromonas palmitatis* sp. nov., a marine dissimilatory Fe(III) reducer. *Arch. Microbiol.* **164**:406–413.
- Coleman, M. L., D. B. Hedrick, D. R. Lovley, D. C. White, and K. Pye. 1993. Reduction of Fe(III) in sediments by sulfate-reducing bacteria. *Nature* **361**:436–438.
- de Man, J. C. 1975. The probability of most probable numbers. *Eur. J. Appl. Microbiol.* **1**:67–78.

19. **Detmers, J.** 1997. Dissimilatorisch-Fe(III)-reduzierende Bakterien—eine mikrobiologisch-ökologische Untersuchung. M.S. thesis, University of Bremen, Bremen, Germany.
20. **Ehrlich, H. L.** 1993. Electron transfer from acetate to the surface of MnO<sub>2</sub> particles by a marine bacterium. *J. Ind. Microbiol.* **12**:121–128.
21. **Finster, K., J. D. Coates, W. Liesack, and N. Pfennig.** 1997. *Desulfuromonas thiophila* sp. nov., a new obligately sulfur-reducing bacterium from anoxic freshwater sediment. *Int. J. Syst. Bacteriol.* **47**:754–758.
22. **Fossing, H., and B. B. Jørgensen.** 1989. Measurement of bacterial sulfate reduction in sediments: evaluation of a single-step chromium reduction method. *Biogeochemistry* **8**:223–245.
23. **Hall, P. O. J., and R. C. Aller.** 1992. Rapid small-volume flow injection analysis for  $\Sigma\text{CO}_2$  and  $\text{NH}_4^+$  in marine and freshwaters. *Limnol. Oceanogr.* **37**:1113–1119.
24. **Harms, G., K. Zengler, R. Rabus, F. Aekersberg, D. Minz, R. Rosselló-Móra, and F. Widdel.** 1999. Anaerobic oxidation of *o*-xylene, *m*-xylene, and homologous alkylbenzenes by new types of sulfate-reducing bacteria. *Appl. Environ. Microbiol.* **65**:999–1004.
25. **Jørgensen, B. B.** 1978. A comparison of methods for the quantification of bacterial sulfate reduction in coastal marine sediments. I. Measurement with radiotracer techniques. *Geomicrobiol. J.* **1**:11–27.
26. **Kostka, J. E., D. E. Canfield, and B. Thamdrup.** 1999. Rates and pathways of carbon oxidation in permanently cold Arctic sediments. *Mar. Ecol. Prog. Ser.* **180**:7–21.
27. **Kristensen, E., A. H. Devol, and H. E. Hartnett.** 1999. Organic matter diagenesis in sediments on the continental shelf and slope of the Eastern Tropical and temperate North Pacific. *Cont. Shelf Res.* **19**:1331–1351.
28. **Kristensen, E., and K. Hansen.** 1995. Decay of plant detritus in organic-poor marine sediment: production rates and stoichiometry of dissolved C and N compounds. *J. Mar. Res.* **53**:675–702.
29. **Laverman, A. M., J. S. Blum, J. K. Schaefer, E. J. P. Phillips, D. R. Lovley, and R. S. Oremland.** 1995. Growth of strain SES-3 with arsenate and other diverse electron acceptors. *Appl. Environ. Microbiol.* **61**:3556–3561.
30. **Li, Y.-H., and S. Gregory.** 1974. Diffusion of ions in sea water and in deep-sea sediments. *Geochim. Cosmochim. Acta* **38**:703–714.
31. **Llobet-Brossa, E., R. Rosselló-Móra, and R. Amann.** 1998. Microbial community composition of Wadden Sea sediments as revealed by fluorescence in situ hybridization. *Appl. Environ. Microbiol.* **64**:2691–2696.
32. **Lonergan, D. J., H. L. Jenter, J. D. Coates, E. J. P. Phillips, T. M. Schmidt, and D. R. Lovley.** 1996. Phylogenetic analysis of dissimilatory Fe(III)-reducing bacteria. *J. Bacteriol.* **178**:2402–2408.
33. **Lord, C. J., III.** 1980. The chemistry and cycling of iron, manganese, and sulfur in salt marsh sediments. Ph.D. thesis, University of Delaware, Newark.
34. **Lovley, D. R.** 1991. Dissimilatory Fe(III) and Mn(IV) reduction. *Microbiol. Rev.* **55**:259–287.
35. **Lovley, D. R., J. D. Coates, D. A. Saffarini, and D. J. Lonergan.** 1997. Dissimilatory iron reduction, p. 187–215. *In* G. Winkelmann and C. J. Carrano (ed.), *Transition metals in microbial metabolism*. Harwood Academic Publishers, Amsterdam, The Netherlands.
36. **Lovley, D. R., and S. Goodwin.** 1988. Hydrogen concentrations as an indicator of the predominant terminal electron-accepting reactions in aquatic sediments. *Geochim. Cosmochim. Acta* **52**:2993–3003.
37. **Lovley, D. R., and E. J. P. Phillips.** 1987. Competitive mechanisms for inhibition of sulfate reduction and methane production in the zone of ferric iron reduction in sediments. *Appl. Environ. Microbiol.* **53**:2636–2641.
38. **Lovley, D. R., and E. J. P. Phillips.** 1988. Manganese inhibition of microbial iron reduction in anaerobic sediments. *Geomicrobiol. J.* **6**:145–155.
39. **Lovley, D. R., and E. J. P. Phillips.** 1986. Organic matter mineralization with reduction of ferric iron in anaerobic sediments. *Appl. Environ. Microbiol.* **51**:683–689.
40. **Lovley, D. R., E. E. Roden, E. J. P. Phillips, and J. C. Woodward.** 1993. Enzymatic iron and uranium reduction by sulfate-reducing bacteria. *Mar. Geol.* **113**:41–53.
41. **Ludwig, W., O. Strunk, S. Klugbauer, N. Klugbauer, M. Weizenegger, J. Neumaier, M. Bachleitner, and K.-H. Schleifer.** 1998. Bacterial phylogeny based on comparative sequence analysis. *Electrophoresis* **19**:554–568.
42. **Maidak, B. L., J. R. Cole, C. T. Parker, Jr., G. M. Garrity, N. Larsen, B. Li, T. G. Lilburn, M. J. McCaughey, G. J. Olsen, R. Overbeek, S. Pramanik, T. M. Schmidt, J. M. Tiedje, and C. R. Woese.** 1999. A new version of the RDP (Ribosomal Database Project). *Nucleic Acids Res.* **27**:171–173.
43. **McClung, C. R., and D. G. Patriquin.** 1980. Isolation of a nitrogen-fixing *Campylobacter* species from the roots of *Spartina alterniflora* Loisel. *Can. J. Microbiol.* **26**:881–886.
44. **McClung, C. R., D. G. Patriquin, and R. E. Davis.** 1983. *Campylobacter nitrofigilis* sp. nov., a nitrogen-fixing bacterium associated with roots of *Spartina alterniflora* Loisel. *Int. J. Syst. Bacteriol.* **33**:605–612.
45. **Millero, F. J.** 1996. *Chemical oceanography*, 2nd ed. CRC Press, Boca Raton, Fla.
46. **Murray, J. W.** 1974. The surface chemistry of hydrous manganese dioxide. *J. Colloid Interface Sci.* **46**:357–371.
47. **Myers, C. R., and K. H. Nealson.** 1988. Microbial reduction of manganese oxides: interactions with iron and sulfur. *Geochim. Cosmochim. Acta* **52**:2727–2732.
48. **Nealson, K. H., C. R. Myers, and B. B. Wimpsee.** 1991. Isolation and identification of manganese-reducing bacteria and estimates of microbial Mn(IV)-reducing potential in the Black Sea. *Deep-Sea Res.* **38**:S907–S920.
49. **Overnell, J., S. M. Harvey, and R. J. Parkes.** 1996. A biogeochemical comparison of sea loch sediments. Manganese and iron contents, sulphate reduction and oxygen uptake rates. *Oceanol. Acta* **19**:41–55.
50. **Parkhurst, D. L.** 1995. Users guide to PHREEQC - a computer program for speciation, reaction-path, advective transport, and inverse geochemical calculations. Water-resources investigations report 95-4227. U.S. Geological Survey, Lakewood, Colo.
51. **Postma, D.** 1985. Concentrations of Mn and separation from Fe in sediments. 1. Kinetics and stoichiometry of the reaction between birnessite and dissolved Fe(II) at 10°C. *Geochim. Cosmochim. Acta* **49**:1023–1033.
52. **Rasmussen, H., and B. B. Jørgensen.** 1992. Microelectrode studies of seasonal oxygen uptake in a coastal sediment: role of molecular diffusion. *Mar. Ecol. Progr. Ser.* **81**:289–303.
53. **Ravenschlag, K., K. Sahn, J. Pernthaler, and R. Amann.** 1999. High bacterial diversity in permanently cold marine sediments. *Appl. Environ. Microbiol.* **65**:3982–3989.
54. **Roden, E. E., and R. G. Wetzel.** 1996. Organic carbon oxidation and suppression of methane production by microbial Fe(III) oxide reduction in vegetated and unvegetated freshwater wetland sediments. *Limnol. Oceanogr.* **41**:1733–1748.
55. **Rosselló-Móra, R., B. Thamdrup, H. Schäfer, R. Weller, and R. Amann.** 1999. The response of the microbial community of marine sediments to organic carbon input under anaerobic conditions. *Syst. Appl. Microbiol.* **22**:237–248.
56. **Rysgaard, S., B. Thamdrup, N. Risgaard-Petersen, H. Fossing, P. Berg, P. B. Christensen, and T. Dalsgaard.** 1998. Seasonal carbon and nutrient mineralization in a high-Arctic coastal marine sediment, Young Sound, Northeast Greenland. *Mar. Ecol. Progr. Ser.* **175**:261–276.
57. **Sahn, K., and U.-G. Berninger.** 1998. Abundance, vertical distribution, and community structure of benthic prokaryotes from permanently cold marine sediments (Svalbard, Arctic Ocean). *Mar. Ecol. Progr. Ser.* **165**:71–80.
58. **Schmidt, J. L., J. W. Deming, P. A. Jumars, and R. G. Keil.** 1998. Constancy of bacterial abundance in surficial marine sediments. *Limnol. Oceanogr.* **53**:976–982.
59. **Schwertmann, U., and R. M. Cornell.** 1991. Iron oxides in the laboratory. VCH, Weinheim, Germany.
60. **Sørensen, J.** 1982. Reduction of ferric iron in anaerobic, marine sediment and interaction with reduction of nitrate and sulfate. *Appl. Environ. Microbiol.* **43**:319–324.
61. **Stoltz, J. F., D. J. Ellis, J. Switzer Blum, D. Ahmann, D. R. Lovley, and R. S. Oremland.** 1999. *Sulfurospirillum* sp. nov. and *Sulfurospirillum arsenophilum* sp. nov., new members of the *Sulfurospirillum* clade of the epsilon *Proteobacteria*. *Int. J. Syst. Bacteriol.* **49**:1177–1180.
62. **Stookey, L. L.** 1970. Ferrozine—a new spectrophotometric reagent for iron. *Anal. Chem.* **42**:779–781.
63. **Sundby, B., and N. Silverberg.** 1981. Pathways of manganese in an open estuarine system. *Geochim. Cosmochim. Acta* **45**:293–307.
64. **Teske, A., P. Sigalevich, Y. Cohen, and G. Muyzer.** 1996. Molecular identification of bacteria from a coculture by denaturing gradient gel electrophoresis of 16S ribosomal DNA fragments as a tool for isolation in pure cultures. *Appl. Environ. Microbiol.* **62**:4210–4215.
65. **Thamdrup, B.** 2000. Microbial manganese and iron reduction in aquatic sediments. *Adv. Microb. Ecol.* **16**:41–84.
66. **Thamdrup, B., and D. E. Canfield.** 2000. Benthic respiration in aquatic sediments, p. 86–103. *In* O. Sala, H. Mooney, R. Jackson, and R. Howarth (ed.), *Methods in ecosystem science*. Springer, New York, N.Y.
67. **Thamdrup, B., and D. E. Canfield.** 1996. Pathways of carbon oxidation in continental margin sediments off central Chile. *Limnol. Oceanogr.* **41**:1629–1650.
68. **Thamdrup, B., H. Fossing, and B. B. Jørgensen.** 1994. Manganese, iron, and sulfur cycling in a coastal marine sediment, Aarhus Bay, Denmark. *Geochim. Cosmochim. Acta* **58**:5115–5129.
69. **Vandamme, P., M. Vancanneyt, B. Pot, L. Mels, B. Hoste, D. Dewettinck, L. Vlaes, C. Van Den Borre, R. Higgins, J. Hommez, K. Kersters, J.-P. Butzler, and H. Goossens.** 1992. Polyphasic taxonomic studies of the emended genus *Arcobacter* with *Arcobacter* comb. nov. and *Arcobacter skirrowii* sp. nov., an aerotolerant bacterium isolated from veterinary specimens. *Int. J. Syst. Bacteriol.* **42**:344–356.
70. **Vargas, M., K. Kashefi, E. L. Blunt-Harris, and D. R. Lovley.** 1998. Microbiological evidence for Fe(III) reduction on early Earth. *Nature* **395**:65–67.
71. **Widdel, F., and F. Bak.** 1991. Gram-negative mesophilic sulfate-reducing bacteria, p. 3352–3378. *In* A. Balows, H. G. Trüper, M. Dworkin, W. Harder, and K.-H. Schleifer (ed.), *The Prokaryotes*, 2nd ed., vol. IV. Springer, New York, N.Y.